

show a favorable intensity ratio of the corresponding features. However, the band positions of the ionized species are shifted only slightly [ $80 \text{ cm}^{-1}$  or less (20)] with respect to the neutrals. It still remains to be shown that ionized gaseous PAHs do not carry the strong 5- to 6- $\mu\text{m}$  emission.

Fulara *et al.* (26) have measured the near-IR, visible, and UV spectra emission from a different class of molecules, highly unsaturated hydrocarbons [ $\text{C}_n\text{H}_m$ ,  $n = 2 - 12$  (even),  $m < 3$ ]. They showed that the near-IR and visible features correspond to 15 DIBs. However, the absorption lines in the UV are inconsistent with astronomical observations. Nevertheless, this class of molecules also should be considered as possible carriers of the UIRs. IR emission spectra of these species as well as emission spectra from large neutral PAHs (for example, coronene or larger) and ionized PAHs must be measured to further explore the possible connections of these molecules with the UIRs and DIBs.

#### REFERENCES AND NOTES

- C. Joblin, J. P. Maillard, L. d'Hendecourt, A. Leger, *Nature* **346**, 729 (1990).
- L. J. Allamandola, A. G. G. M. Tielens, J. R. Barker, *Astrophys. J. Suppl.* **71**, 733 (1989).
- T. R. Geballe, in *Proceedings of the Workshop on Laboratory and Observational Infrared Spectra of Interstellar Dust*, Hilo, HI, USA, 18 to 20 July 1983, R. D. Wolstencroft and J. M. Greenberg, Eds., *R. Obs. Occas. Rep.* **12**, 93 (1984); R. W. Russel, B. T. Soifer, S. P. Willner, *Astrophys. J.* **217**, L149 (1977).
- T. R. Geballe, J. H. Lacy, S. E. Persson, P. J. McGregor, B. T. Soifer, *Astrophys. J.* **292**, 500 (1985).
- M. Cohen *et al.*, *ibid.* **302**, 737 (1986).
- J. D. Bregman, L. J. Allamandola, A. G. G. M. Tielens, T. R. Geballe, F. C. Witteborn, *ibid.* **344**, 791 (1989).
- S. P. Willner, B. T. Soifer, R. W. Russel, R. R. Joyce, F. C. Gillet, *ibid.* **217**, L121 (1977); F. C. Gillet, D. E. Kleinmann, E. L. Wright, R. W. Capps, *ibid.* **198**, L65 (1975).
- A. Leger and J. L. Puget, *Astron. Astrophys.* **137**, L5 (1984); L. J. Allamandola, A. G. G. M. Tielens, J. R. Barker, *Astrophys. J.* **290**, L25 (1985).
- S. J. Clemett, C. R. Maechling, R. N. Zare, P. D. Swan, R. M. Walker, *Science* **262**, 721 (1993); L. J. Allamandola, S. A. Sandford, B. Wopenka, *ibid.* **237**, 56 (1987).
- J. D. Brenner and J. R. Barker, *Astrophys. J.* **388**, L39 (1992).
- I. Cherchneff and J. R. Barker, *ibid.* **341**, L21 (1989).
- J. Shan, A. Suto, L. C. Lee, *ibid.* **383**, 459 (1991); J. Shan, M. Suto, L. C. Lee, *J. Photochem. Photobiol. A: Chem.* **63**, 139 (1992).
- S. Schlemmer *et al.*, in preparation.
- R. M. Williams and S. R. Leone, *Astrophys. J.*, in preparation.
- J. Harrison *et al.*, in preparation.
- M. D. Petroff, M. G. Stapelbroek, W. A. Kleinhans, *Appl. Phys. Lett.* **51**, 406 (1985).
- A. Leger and H. d'Hendecourt, *Ann. Phys. Fr.* **14**, 181 (1989).
- M. Buck and P. Hess, *Appl. Surf. Sci.* **43**, 358 (1989).
- W. A. Schutte, A. G. G. M. Tielens, L. J. Allamandola, *Astrophys. J.* **415**, 397 (1993).
- J. Szczepanski and M. Vala, *Nature* **363**, 699 (1993); *Astrophys. J.* **413**, 646 (1993).
- L. J. Allamandola *et al.*, *Astrophys. J.* **345**, L59 (1989).
- D. C. B. Whittet, A. D. McFadzean, T. R. Geballe, *R. Astron. Soc. Mon. Not.* **211**, 29 (1984); D. C. B. Whittet *et al.*, *ibid.* **233**, 321 (1988); D. K. Aitken and P. F. Roche, *ibid.* **196**, 39 (1981); T. R. Geballe, K. S. Noll, D. C. B. Whittet, L. B. F. M. Waters, *Astrophys. J.* **340**, L29 (1989); R. W. Russel, B. T. Soifer, S. P. Willner, *ibid.* **220**, 568 (1978); W. A. Schutte, A. G. G. M. Tielens, L. J. Allamandola, M. Cohen, D. H. Wooden, *ibid.* **360**, 577 (1990), and references therein.
- F. Pauzat, D. Talbi, M. D. Miller, D. J. DeFrees, Y. Ellinger, *J. Phys. Chem.* **96**, 7882 (1992).
- J. R. Barker, *ibid.*, p. 7361.
- D. M. Hudgins, S. A. Sandford, L. J. Allamandola, *ibid.* **98**, 4243 (1994).
- J. Fulara, D. Lessen, P. Freivogel, J. P. Maier, *Nature* **366**, 439 (1993).

27. This work was funded by the National Aeronautics and Space Administration (NASA) Exobiology Program (grant NAGW-2763) and the NASA Astrophysics Program (grant #NAGW-2991). S.S. thanks the Deutsche Forschungsgemeinschaft for a research fellowship. D.J.C. thanks the California Space Institute for a fellowship. We acknowledge the efforts of the late Professor George C. Pimentel in initiating the photon counting experiment. Rockwell supplied the single-photon counting detector, and we acknowledge the enthusiastic cooperation of M. Petroff. We thank C. B. Moore for carefully reading the manuscript.

13 April 1994; accepted 20 July 1994

## X-ray Variability in the Hot Supergiant $\zeta$ Orionis

Thomas W. Berghöfer and Jürgen H. M. M. Schmitt

Hot massive stars represent only a small fraction of the stellar population of the galaxy, but their enormous luminosities make them visible over large distances. Therefore, they are ideal standard candles, used to determine distances of near galaxies. Their mass loss due to supersonic winds driven by radiation pressure contributes significantly to the interstellar medium and thus to the chemical evolution of galaxies. All hot stars are soft x-ray sources; in contrast to the sun with its highly variable x-ray flux, long time scale x-ray variability is not common among hot stars. An analysis is presented here of an unusual increase in x-ray flux observed with the roentgen observatory satellite during a period of 2 days for the hot supergiant  $\zeta$  Orionis, the only episode of x-ray variability that has been found in a hot star. These observations provide the most direct evidence so far for the scenario of shock-heated gas in the winds of hot stars.

X-ray observations carried out with the Einstein Observatory (1) and the roentgen observatory satellite (ROSAT) (2) have shown that all hot stars are soft x-ray sources with  $\approx 10^{-7}$  (the typical range for the solar value is  $10^{-7}$  to  $10^{-6}$ ) of their total luminosity emitted as soft x-rays (1–3). Early attempts to explain the observed x-ray emission in hot stars by a thin, hot corona at the base of the wind (4), similar to the solar x-ray corona, have become untenable. First, the absorption of the x-ray emission by the overlying wind requires an enormous emission measure of x-ray-emitting material (5). However, the search for the green corona emission line (Fe XIV, 530.3 nm), which is a direct indicator of gas at coronal temperatures, in the optical spectra of hot stars has been unsuccessful (6) and could not provide any observational evidence for the existence of hot gas in massive stars. Second, x-ray spectra of hot stars show no evidence for absorption at the 0.6-keV K shell ionization edge of oxygen (7) predicted in coronal models. Third, in contrast to cool stars like our sun, with its highly variable coronal activity, our long-term x-ray variability studies provide no evidence for x-ray time variability for hot stars over time scales of up to several years (2, 8).

The theory of stellar winds driven by line radiation (9, 10), developed to explain the mass loss from hot stars, provides a different mechanism for the generation of x-rays in hot stars: The winds of hot stars are driven by the absorption of stellar radiation in a multitude of ultraviolet spectral lines, and stability analyses show that such line-driven winds are extremely unstable (11). In a more phenomenological way, Lucy and White (12) postulated (as a consequence of these instabilities) the presence of hot gas (and hence the x-ray emission) generated by shocks in the hot star winds. Detailed time-dependent calculations (13) show that the growth of instabilities naturally leads to the production of strong shocks that arise from the deceleration of high-speed wind material that impacts on slower material (thus driving a reverse shock). The combination of this effect with the results of our long-term x-ray variability studies of hot stars (2, 8), which indicate that the x-ray emission of hot stars remains very constant over long time scales, makes it seem likely that the observed x-ray emission is the average output from a larger number of shocks distributed in the wind of these stars.

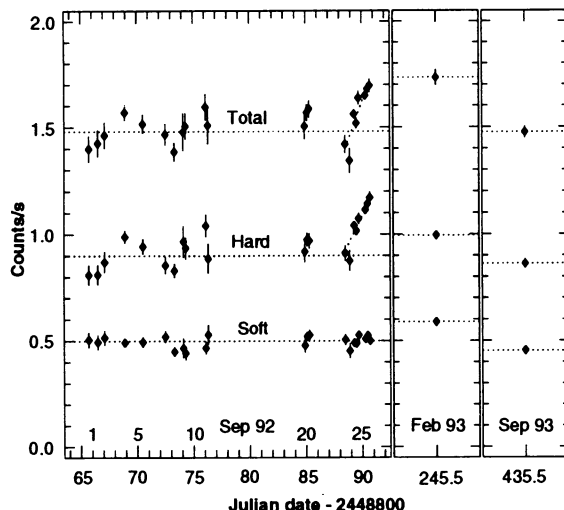
A recently obtained ROSAT position sensitive proportional counter (PSPC) spectrum of the hot prototype star  $\zeta$  Puppis (14) clearly shows the "self-absorption" of

Max-Planck-Institut für Extraterrestrische Physik, 85740 Garching bei München, Germany.

the observed x-ray emission by the stellar wind; the PSPC spectrum can be explained by the assumption that the x-ray emission arises from hot shocks distributed throughout a cool wind. However, all model calculations for such a scenario are based on assumed shock structures; the only method to check these assumptions is the search for time variability in the x-ray output of these stars.

The star  $\zeta$  Orionis has been multiply observed with the PSPC onboard the ROSAT (15–17). In this report, we concentrate on the observations of  $\zeta$  Orionis during September 1992 and thereafter; during the observations from September 1990 to September 1992, the x-ray emission of  $\zeta$  Orionis remained at a constant flux level (8). In Fig. 1, we present the x-ray light curve of  $\zeta$  Orionis, which had its background subtracted and was corrected by vignetting, that was observed during this time in the total (0.1 to 2.5 keV), hard (0.65 to 2.4 keV), and soft (0.15 to 0.51 keV) energy bands. The x-ray count rate in the hard band (and therefore in the total band) increased by  $\approx 30\%$  from the value on 23 to 25 September 1992 (Fig. 1). During the observations in February 1993 and September 1993, the count rate in the hard energy band decreased to a value consistent with the count rate before the observed increase in September 1992. Until the end of September 1992, the count rate in the soft energy band did not vary at all. Compared to September 1992 values in February 1993 the x-ray count rate in the soft energy band is enhanced by  $\approx 20\%$  and decreased in September 1993 to a value that is consistent with the observed rate in September 1992. Thus, in September 1993  $\zeta$  Orionis showed the same flux levels in all of ROSAT's energy bands as before the increase in September 1992.

**Fig. 1.** The x-ray light curves (total, hard, and soft ROSAT bands) of  $\zeta$  Orionis during September 1992 (Sep 92), February 1993 (Feb 93), and September 1993 (Sep 93).



The scenario for x-ray production in hot stars indicates that the enhanced x-ray emission of  $\zeta$  Orionis is a strong shock wave propagating and cooling in the wind. On the basis of model calculations (13), one would expect the x-ray emission to arise when fast-moving rarefied material impacts on more slowly moving, denser shells. For simplicity, we model this heated post-shock gas as an expanding shell in the stellar wind and calculate the spherically symmetric radiative transfer for the x-ray emission in an expanding shell absorbed by the cool overlying wind. Ignoring for the moment any change in the underlying wind speed, we adopt a wind density,  $n_{\text{wind}}$ , scaling with radius  $r$  as  $n_{\text{wind}} = n_0 r_0^2 / r^2$  and a shell density (of the post-shock gas) as

$$n_{\text{shell}}(r) = C_1 \cdot (n_0 r_0^2 / r_{\text{shell}}^2) \delta(r - r_{\text{shell}}) \quad (1)$$

where  $n_0 = \dot{M} / (4\pi\mu v_{\text{wind}} r_0^2)$  denotes the wind density at some reference radius  $r_0$ ,  $r_{\text{shell}}$  is the shell radius,  $v_{\text{wind}}$  is the wind velocity,  $C_1$  and  $C_2$  (below) are constant scaling factors, and  $\mu$  is the mean ionic weight. On the assumption of optically thin emission, the emission measure  $EM$  of the shell scales as

$$EM_{\text{shell}} \propto C_2 \cdot n_{\text{shell}}^2 4\pi r_{\text{shell}}^2 \Delta r \propto r_{\text{shell}}^{-2} \Delta r \quad (2)$$

In our simplified model, the whole problem can be characterized by one single dimensionless parameter given by the radius of the shell  $r_{\text{shell}}$  divided by the distance,  $r_{\tau=1}$ , where the optical depth,  $\tau$ , along the line of sight toward the center of the star becomes unity. The resulting flux of the shell,  $f_{\text{shell}}$ , then becomes

$$f_{\text{shell}} = f(r_{\text{shell}}/r_{\tau=1}) = \int dEM_{\text{shell}} \cdot e^{-\tau_{\text{wind}}} \quad (3)$$

where  $\tau_{\text{wind}}$  denotes the optical depth from

a given shell element to infinity. Figure 2 schematically illustrates three stages of the expanding shell and the resulting x-ray flux: As long as the shell is close to the stellar surface (solid line), the optical depth is large and no radiation can escape. As the shell expands (long dashed line), larger and larger fractions of the shell become visible and hence the x-ray flux increases. Finally, in the late stages of expansion (short-dashed line) the x-ray flux decreases again because  $EM_{\text{shell}} \propto r^{-2}$ .

The basic idea relating the above model to our observations is that each point in time is associated with some shell radius by the choice of a suitable expansion velocity. We fitted the observed 2-day increase in the hard x-ray band to this model and deduced from the best fit (Fig. 2) of the shell radius after 2 days a shell velocity of

$$v_{\text{shell}} = \left( \begin{matrix} +50 \\ 76 \\ -26 \end{matrix} \right) \cdot \frac{r_{\tau=1}}{R_*} \text{ km/s} \quad (4)$$

where

$$r_{\tau=1} = \frac{\dot{M}\sigma}{4\pi\mu v_{\text{wind}}} \quad (5)$$

Note that our best fit model requires that the observed increase falls in the linearly

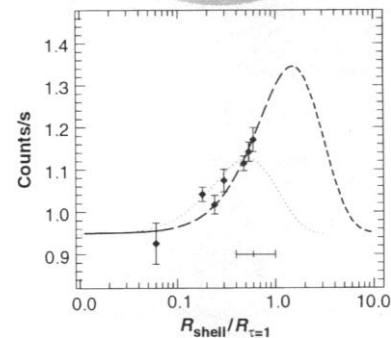
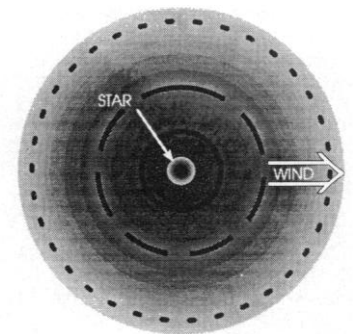


**Fig. 2.** (Top) Model of an expanding shell of post-shock gas in the stellar wind. Solid, long-dashed, and short-dashed lines represent three different stages of the expanding shell. (Bottom) Model fit to the increase in the hard ROSAT band of  $\zeta$  Orionis (horizontal error bar indicates the best fit with its uncertainties of the shell radius after 2 days). The dotted line shows the best fit for the case in which the shell is forced to the same velocity as that of the wind.

increasing part of our model, and so the maximal x-ray flux is not yet reached after 2 days. Expressed in physical units, the shell velocity depends on the mass loss rate,  $\dot{M}$ , the wind velocity,  $v_{\text{wind}}$ , in the x-ray-emitting region, and the energy-dependent absorption coefficient,  $\sigma$ , of the absorbing wind material.

For  $r_{\tau=1}/R_* = 7.5$ , which is the mean radius of optical depth unity for the wind properties of  $\zeta$  Orionis (8) in the energy range of 0.6 to 1.0 keV, where the enhanced x-ray emission appeared during the first 2 days, we derive a best-fit shell velocity of 570 km/s. From the analytical velocity field  $v(r) = v_\infty(1 - R_*/r)^\beta$ , which describes the velocity of the smooth wind in an O-type star, we determine a wind velocity of 1600 km/s in the vicinity of the shell after 2 days. Therefore, in the star's frame the post-shock gas moves outward but more slowly than the ambient wind (reverse shock). Using again 1600 km/s (in the star frame) as the characteristic speed of unshocked wind material entering the shock, we deduce a shock velocity of  $\approx 1000$  km/s (in the star frame), which is consistent with the temperature of the x-ray-emitting material derived from a spectral fit of our PSPC data, given the errors of the deduced shock velocity.

We emphasize that a model of a shell propagating with the velocity of the ambient wind (thin dotted line in Fig. 2) cannot fit the observed increase in x-ray count rate. Such a model would lead to an increase and a disappearance of the shell's x-ray emission that are much faster than those observed. With our model of a propagating shock in the wind, we can explain the observed increase in x-ray count rate observed for  $\zeta$  Orionis. The result of our calculations for the flow of the post-shock gas in the stellar wind of  $\zeta$  Orionis confirms the results of the wind models that predict that reverse shocks in stellar winds are much stronger than forward shocks. Our ROSAT observations of  $\zeta$  Orionis provide the first direct observational evidence for the existence of propagating shock waves in the winds of hot stars.

## REFERENCES AND NOTES

1. T. Chlebowski, F. R. Hamden Jr., S. Sciortino, *Astrophys. J.* **341**, 427 (1989).
2. T. W. Berghöfer and J. H. M. M. Schmitt, in *Proceedings of the International Astrophysical Union Symposium 162 on Pulsation, Rotation and Mass Loss in Early-Type Stars*, L. Balona et al., Eds. (Kluwer, Dordrecht, the Netherlands, 1993).
3. K. S. Long and R. L. White, *Astrophys. J.* **239**, L65 (1980).
4. J. P. Cassinelli and G. L. Olson, *ibid.* **229**, 304 (1979).
5. W. L. Waldron, *ibid.* **282**, 256 (1984).
6. D. Baade and L. B. Lucy, *Astron. Astrophys.* **178**, 213 (1987).
7. J. P. Cassinelli and J. H. Swank, *Astrophys. J.* **271**, 681 (1983).
8. T. W. Berghöfer and J. H. M. M. Schmitt, *Astron. Astrophys.*, in press.
9. L. B. Lucy and P. M. Solomon, *Astrophys. J.* **159**, 879 (1970).
10. J. L. Castor, D. C. Abbott, R. I. Klein, *ibid.* **195**, 157 (1975).
11. K. B. MacGregor, L. Hartmann, J. C. Raymond, *ibid.* **231**, 514 (1979).
12. L. B. Lucy and R. L. White, *ibid.* **241**, 300 (1980).
13. S. P. Owocki, J. I. Castor, G. B. Rybicki, *ibid.* **335**, 914 (1988).
14. D. J. Hillier et al., *Astron. Astrophys.* **276**, 117 (1993).
15. J. Trümper, *Adv. Space Res.* **2** (4), 241 (1983).
16. J. Trümper et al., *Nature* **349**, 579 (1991).
17. E. Pfeiffermann et al., *Soc. Photoopt. Instrum. Eng.* **733**, 519 (1986).
18. The ROSAT project has been supported by the Bundesministerium für Forschung und Technologie (BMFT) and the Max-Planck-Gesellschaft (MPG). We acknowledge the support of our colleagues from the ROSAT group and thank A. Feldmeier for a copy of his doctoral thesis, which has given us useful information and inspiration for the interpretation of the presented x-ray data.

2 May 1994; accepted 29 July 1994

## Stabilization of Atomic Hydrogen in Both Solution and Crystal at Room Temperature

Riichi Sasamori, Yoshihiro Okaue, Toshiyuki Isobe, Yoshihisa Matsuda\*

Atomic hydrogen has been stably encapsulated in both solution and crystal at room temperature. Upon  $\gamma$ -ray irradiation of  $[(\text{CH}_3)_3\text{Si}]_8\text{Si}_8\text{O}_{20}$ , which is the trimethylsilylated derivative of the silicate anion with a double four-ring (D4R) cage, electron spin resonance (ESR) spectra revealed that a single hydrogen atom is encapsulated in the center of the D4R cage and is stable for periods of many months. Attack by chemically reactive species such as oxygen was prevented by the D4R cage, but the ESR signal of the hydrogen atom was sensitive to the magnetic interaction caused by the presence of the  $\text{O}_2$  molecule near the cage.

The hydrogen atom, the simplest of atoms and free radicals, is difficult to trap at ambient temperature because of its high activity and small size. Electron spin resonance has been used to study hydrogen atoms in several matrices, including KCl,  $\text{CaF}_2$ , quartz, rare gas ices, and acid ices (1). In these matrices, the ESR signals of atomic hydrogen were observed only at low temperatures such as 4.2 and 77 K because the trapped hydrogen was unstable. In some cases, after the matrix was warmed to room temperature for a few minutes and cooled again, the signal disappeared (2). On the other hand, there is an example of an x-ray-irradiated human tooth in which atomic hydrogen is stabilized at room temperature in an inorganic medium (3). However, the above hydrogen radical centers have not been made in a compound with a cage structure, which can encapsulate a single hydrogen atom and protect it against the reactive surroundings. In our study, we succeeded in stably trapping atomic hydrogen at room temperature upon  $\gamma$ -ray irradiation of  $[(\text{CH}_3)_3\text{Si}]_8\text{Si}_8\text{O}_{20}$ , which is the trimethylsilylated derivative of silicate anion with a D4R structure. The ESR spectra revealed that atomic hydrogen was present. This hydrogen atom is most likely encapsulated in the center of the D4R framework structure in both solution and crystal for a long time.

The above compound was synthesized by

trimethylsilylation of tetramethylammonium silicate,  $[(\text{CH}_3)_4\text{N}]_8\text{Si}_8\text{O}_{20} \cdot \text{XH}_2\text{O}$  (4). The crystals obtained were analyzed by infrared spectroscopy, elemental analysis, and gas chromatography. The single-crystal x-ray structure analysis, which was performed at room temperature, revealed that the molecule crystallized in the space group  $P\bar{1}$  with one equivalent molecule in the unit cell (observed density,  $D_{\text{O}}$ , of  $1.181 \text{ g cm}^{-3}$ ). Although the  $R$  values, as expected, did not become smaller because of the large temperature factors of the terminal methyl group (5), the core structure of the  $[(\text{CH}_3)_3\text{Si}]_8\text{Si}_8\text{O}_{20}$  could be determined. Figure 1 illustrates the cube-like structure with a cavity at a center in the D4R framework. The average packing distances for neighboring and diagonal Si-Si atoms in the D4R framework are  $3.079 \pm 0.004$ ,  $4.355 \pm 0.004$ , and  $5.329 \pm 0.007 \text{ \AA}$ , respectively. Similarly, the O-O packing distances are  $2.607 \pm 0.009$ ,  $3.687 \pm 0.008$ , and  $5.197 \pm 0.013 \text{ \AA}$ , respectively. A space-filling representation of the structure made by use of the van der Waals radii of silicon and oxygen reveals that a cavity in the D4R cage can encapsulate a hydrogen atom and that the meshes of the D4R cage are much smaller than that of a hydrogen atom.

An ESR spectrum of atomic hydrogen encapsulated in polycrystalline  $[(\text{CH}_3)_3\text{Si}]_8\text{Si}_8\text{O}_{20}$  by irradiation with  $^{60}\text{Co}$   $\gamma$ -rays [ $10^5$  Grays (Gy)] at room temperature is given in Fig. 2A. The ESR spectral feature is similar to that of irradiated quartz at 77 K (2). Two

Department of Chemistry, Faculty of Science, Kyushu University, Higashi-ku, Fukuoka, 812 Japan.

\*To whom correspondence should be addressed.